

Memory Effect in Crystallisation of Amorphous $\text{Ge}_2\text{Sb}_2\text{Te}_5$

R. O. Jones, J. Kalikka, J. Akola

published in

NIC Symposium 2016

K. Binder, M. Müller, M. Kremer, A. Schnurpfeil (Editors)

Forschungszentrum Jülich GmbH,
John von Neumann Institute for Computing (NIC),
Schriften des Forschungszentrums Jülich, NIC Series, Vol. 48,
ISBN 978-3-95806-109-5, pp. 209.
<http://hdl.handle.net/2128/9842>

© 2016 by Forschungszentrum Jülich

Permission to make digital or hard copies of portions of this work for personal or classroom use is granted provided that the copies are not made or distributed for profit or commercial advantage and that copies bear this notice and the full citation on the first page. To copy otherwise requires prior specific permission by the publisher mentioned above.

Memory Effect in Crystallisation of Amorphous $\text{Ge}_2\text{Sb}_2\text{Te}_5$

Robert O. Jones^{1,2}, Janne Kalikka³, and Jaakko Akola^{4,5}

¹ Peter Grünberg Institut PGI-1 and JARA-HPC, Forschungszentrum Jülich,
52425 Jülich, Germany
E-mail: r.jones@fz-juelich.de

² German Research School for Simulation Sciences,
Forschungszentrum Jülich and RWTH Aachen University, 52425 Jülich, Germany

³ Singapore University of Technology and Design, Singapore 487372
E-mail: janne.kalikka@gmail.com

⁴ Department of Physics, Tampere University of Technology, FI-33101, Tampere, Finland
E-mail: jaakko.akola@tut.fi

⁵ COMP Centre of Excellence, Department of Applied Physics, Aalto University,
FI-00076 Aalto, Finland

The rate-limiting process in phase change (PC) optical memories is the extremely rapid (nanosecond time scale) crystallisation of nanosized amorphous “marks” in a polycrystalline layer. Our knowledge of the amorphous and ordered structures of Ge/Sb/Te and Ag/In/Sb/Te alloys has improved significantly in recent years and has led to plausible pictures for the transition between them. Nevertheless, the simulation of the actual crystallisation process is complicated by the need to study large numbers of atoms over time scales that are difficult to attain, even with modern supercomputers. We have performed a series of density functional/ molecular dynamics (DF/MD) simulations on a sample of the prototype PC material $\text{Ge}_2\text{Sb}_2\text{Te}_5$ (GST-225) with 460 atoms. Simulations at 500 K, 600 K, and 700 K have been performed for up to 600 picoseconds in samples where crystallisation was promoted by fixing the structure of a crystalline “seed”, and for over 4 ns in four samples at 600 K without constraints. A comparison of the last four simulations shows a striking memory effect where crystallisation is favoured in an amorphous sample that had previously been crystallised.

1 Introduction

Phase change (PC) materials are chalcogenide alloys (usually Se, Te) that switch very rapidly between the amorphous (a-) and crystalline (c-) phases. They are used extensively in rewritable high-density data storage, especially in optical recording [Digital Versatile Disc (DVD), Blu-ray Disc]¹. Information is stored as rows of nanosized amorphous marks in a polycrystalline layer and accessed via the different optical or electrical properties of the two phases. The most common materials are GeTe-Sb₂Te₃ pseudobinary compounds and Sb-Te binary compounds with small amounts of In, Ag, and/or Ge. Recrystallisation in the two groups is strikingly different, as shown in Fig. 1: In the first [Group 1, Fig. 1(b)] it proceeds mainly via nucleation inside the marks, in the second [Group 2, Fig. 1(c)] via crystal growth from the rim¹. In this report we restrict ourselves to the former.

Close collaboration between theory (density functional/ molecular dynamics simulations) and experiment (particularly x-ray diffraction and EXAFS) has shown that the amorphous structure of $\text{Ge}_2\text{Sb}_2\text{Te}_5$ (GST-225) and other alloys of Ge, Sb, and Te can be

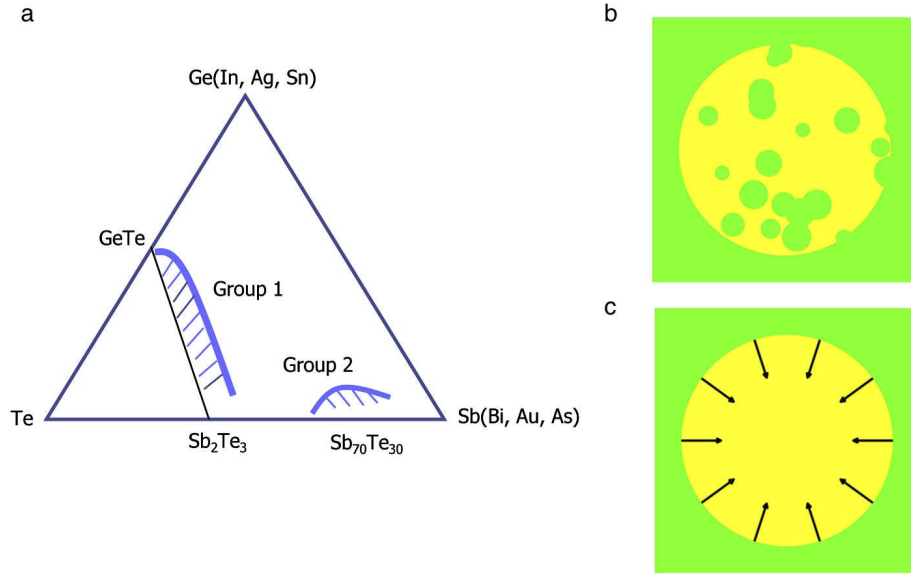


Figure 1. PC materials and their crystallisation patterns. (a) Commonly used materials for optical recording, (b) group 1: Nucleation-dominated (GST), and (c) group 2: growth-dominated recrystallisation (AIST).

characterised by “*ABAB* alternation” (*A*: Ge,Sb, *B*: Te) with four-membered *ABAB* rings being a dominant motif^{2,3}. Since this pattern is prevalent in the metastable (rock salt) crystalline structure, it is plausible that the rapid amorphous-to-crystalline transition be viewed as a re-orientation (nucleation) of disordered *ABAB* squares supported by the space provided by cavities. Knowledge of the amorphous and crystalline structures of an Ag/In/Sb/Te alloy allows us to develop a picture of crystallisation in this case as well⁴. Simulations of crystallisation in GST-225 have been carried out on samples with less than 200 atoms with interesting results^{5,6}, but small samples leave many questions unanswered. We describe here DF/MD simulations of a sample of 460 atoms. In the first simulations, crystallisation is promoted by fixing the structure of a crystalline “seed” (58 atoms, 6 vacancies) throughout. The most recent calculations, referred to below as *run0*–*run3*, there was no seed. In all cases, the densities were adjusted during the simulation to allow for the difference between the amorphous and crystalline forms.

2 Computational Methods

The combined DF/MD calculations were performed on GST-225 with the CPMD program package⁷, using the approximation of Perdew et al. (PBEsol)⁸ for the exchange-correlation energy and scalar-relativistic Troullier-Martins pseudopotentials⁹ with a plane wave cutoff energy of 20 Ry. Periodic boundary conditions were used, with a single point ($k=0$) in the Brillouin zone of the cubic unit cell, and the temperature was controlled by a Nosè-Hoover thermostat.

The initial structures of all simulations were based on the amorphous GST-225 structure of Ref. 3, which agreed well with experimental XRD and XPS measurements. Seven simulations were performed: three with a fixed crystalline seed in the centre of the simulation cell (“fixed-seed runs”)¹⁰, one with an unconstrained seed (*run0*), and three without a seed (*run1*, *run2*, *run3*). The “seeded” starting structure incorporated a $4 \times 4 \times 4$ crystallite (13 Ge, 13 Sb, 32 Te atoms, 6 vacancies, rock salt structure with lattice constant 3.0 Å) into the amorphous structure³. The crystallite had the rock salt structure that is often assumed for GST-225, with Te atoms on one sublattice, and randomly distributed Ge, Sb, and vacancies on the other¹¹. The overlapping atoms were removed, and the structure was relaxed with the atoms of the seed fixed throughout.

The initial structure for *run1* was the original amorphous structure, and those for *run2* and *run3* were derived from this by running 500 MD steps with velocity scaling for *run2*, and another 500 steps for *run3*. The fixed seed runs were performed at 500, 600, and 700 K¹⁰, while all other simulations were at 600 K. The simulation box was adjusted to the change in density ($\sim 7\%$) between the amorphous and crystalline densities by reducing the starting box size (24.629 Å) in five steps of 0.114 Å to the final size (24.06 Å), following the number of crystalline atoms.

The order in the sample was studied using several measures: First, “crystalline” atoms were identified with the aid of the order parameter of Steinhardt, Nelson, and Ronchetti¹², which has proved to be of value in discussing bond orientation order in disordered systems:

$$\bar{Q}_l(i) = \sqrt{\frac{4\pi}{2l+1} \sum_{m=-l}^l |\bar{Q}_{lm}(i)|^2}, \quad (1)$$

where

$$\bar{Q}_{lm}(i) = \frac{1}{N_b(i)} \sum_{k=0}^{N_b(i)} Q_{lm}(k), \quad \text{and} \quad Q_{lm}(i) = \frac{1}{N(i)} \sum_{j=1}^{N(i)} Y_{lm}(\vec{r}_{ij}). \quad (2)$$

$N(i)$ is the number of neighbours for atom i , $N_b(i)$ includes the atom i and its neighbours, and $Y_{lm}(\vec{r}_{ij})$ are spherical harmonics. The first non-zero value of \bar{Q}_ℓ for cubic structures is for $\ell = 4$, and we define “crystalline” atom to be those for which $\bar{Q}_4 \geq 0.6$.

Second, the clustering of such atoms allows us to analyse the individual structures for “percolation”. If we assume a maximum bond length 3.2 Å, a cluster “percolates” if there is a path connecting an atom to its replica in the neighbouring unit cell. We have also studied the changes that occur in the (partial) pair distribution functions, the numbers of “wrong bonds” and *ABAB* squares, the electronic density of states, and the mean square displacement of the atoms.

3 Results and Discussion

The fixed seed simulations at 600 and 700 K crystallised within 600 ps¹⁰, and *run0* crystallised fully within 1.2 ns. The fixed seed run at 500 K showed signs of crystal growth but crystallisation was not complete within 600 ps. Simulations *runs1-3* showed nucleation, and varying degrees of crystal growth within 4 ns with the degree of crystallinity being more than 50% in *run1* and *run2*, and less than 50% in *run3* at that time. More details are provided in Ref. 13.

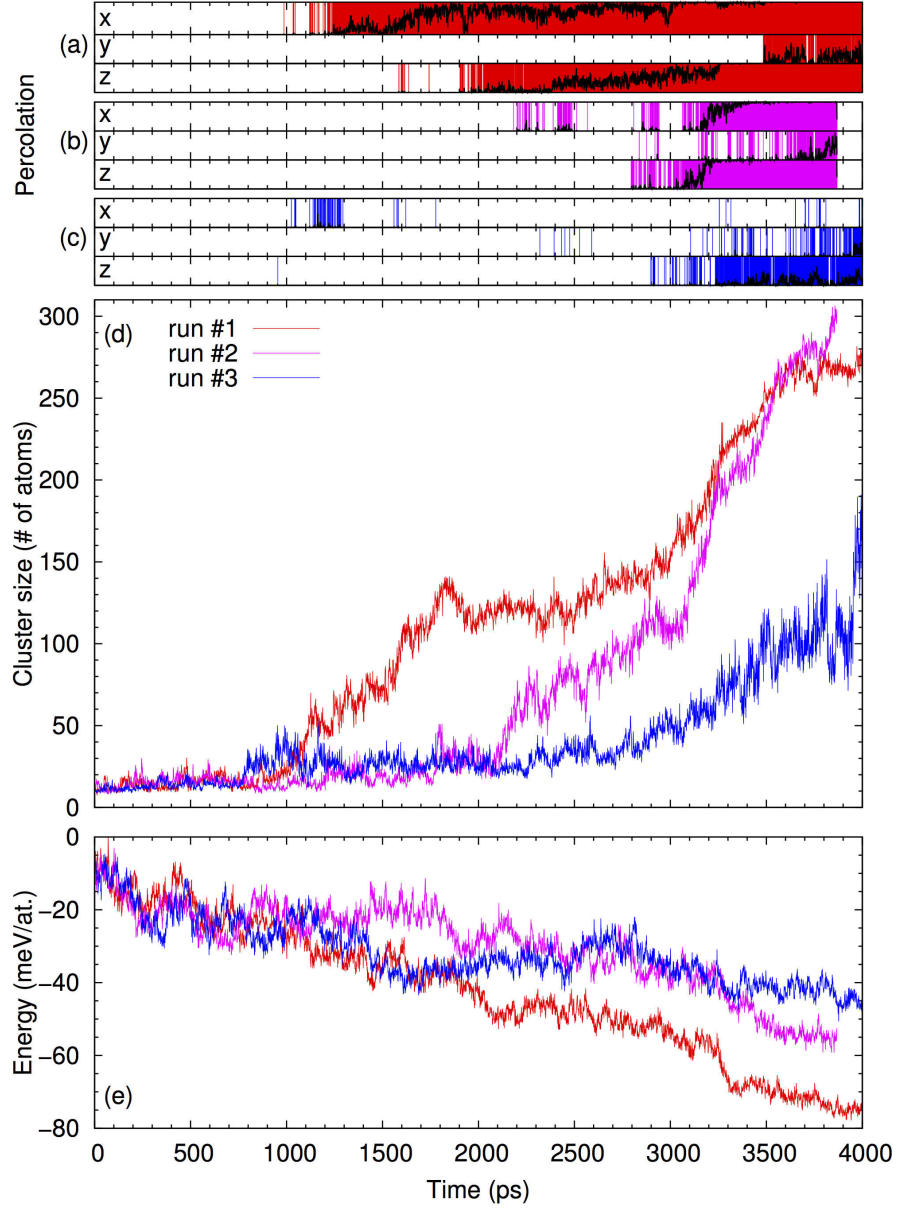


Figure 2. Three simulations (*run1* – *run3*) starting from the amorphous structure of Ref. 3. (a-c) Percolation in x-, y-, and z-directions. Black: fraction of percolating frames in 1 ps windows; coloured background: percolating frames; (d) size of largest cluster; and (e) total energy (normalised for box size). Red: *run1*, purple: *run2*, blue: *run3*.

The early nuclei in *runs0-3* differ significantly in size and shape. The initial nucleus in *run0* grows steadily until crystallisation is complete, while *runs1-3* have subcritical nuclei that fluctuate between 10-50 atoms. The shapes of the nuclei are often stringlike chains of crystalline atoms and isolated ABAB-squares, but more spherical fused blocks of ABAB-cubes (complete or incomplete) are also common. The shapes of the nuclei can differ from the classical nucleation theory picture, and the motifs common in them are AB-alternation and bond angles close to 90 degrees.

In Fig. 2 we plot the crystallisation and percolation properties, as well as the total energies, of *runs1-3*. Percolation is found in *runs0-3* well before the rapid crystallisation phase and can occur with as little as 20% crystallinity. In all these simulations, percolation is initially intermittent in one direction. Sometimes it proceeds along another direction, but in all cases it is more constant later, and extends to two and three dimensions. The rapid crystallisation phase happens during three-dimensional constant percolation in *run0*, and

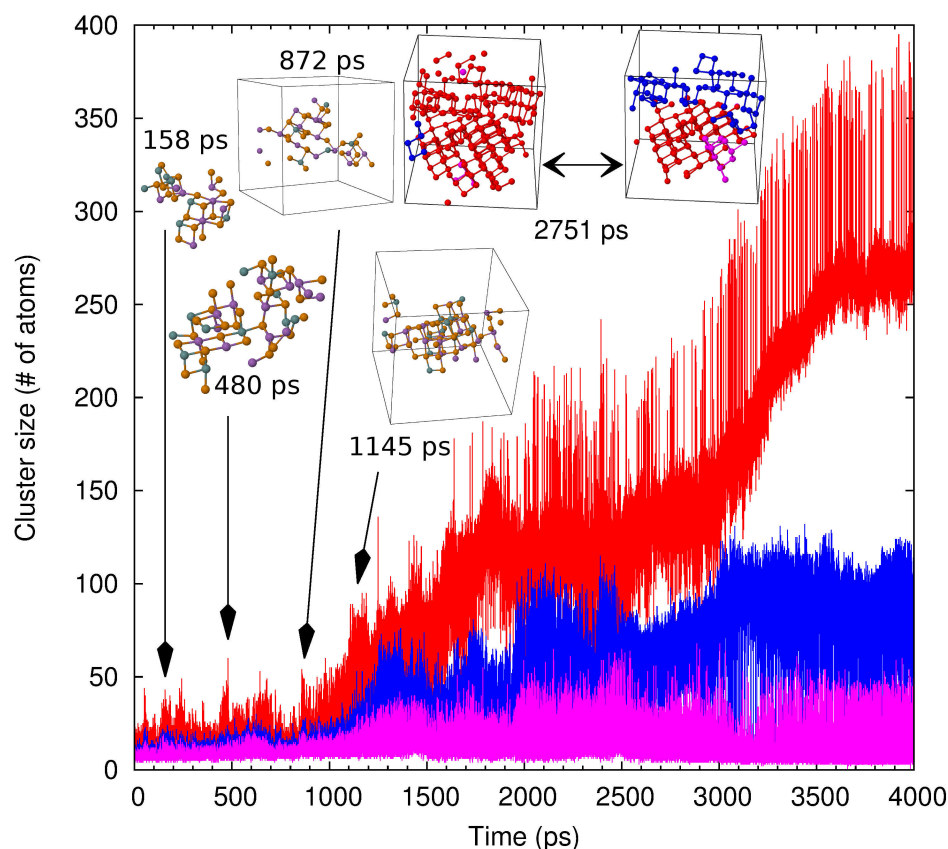


Figure 3. Evolution of the three largest crystalline nuclei of *run1* as a function of time. Red: largest cluster; blue: second largest; purple: third largest. Also shown are the largest crystalline nuclei of *run1* when the size of the largest cluster had a maximum. After ~ 2 ns, the two largest clusters (red, blue) have a fluctuating interface that affects the cluster labelling.

during two-dimensional constant percolation in *run1* and *run2*. In *run3* there is constant percolation in one direction after 2.5 ns, and in two directions just before 4 ns.

The evolution of the size of the crystalline nuclei in *run1* is shown in Fig. 3. The crystal growth rate is low until the critical nucleus size is reached, and then increases until the fraction of crystalline atoms reaches 30-50%. The crystallisation rate in *run2* during the percolating phase is of the order of 1 m/s, which is less than recently measured with differential scanning calorimetry (DSC) at 600 K (2.5-3.0 m/s)¹⁴. After this stage, the structure collapses rapidly until all atoms are crystalline. There is one main crystallite in *run2*, and crystallisation proceeds to completion. In the case of multiple crystallites where none is dominant in size (as in *run1*), crystallisation is incomplete.

Crystallisation takes place within a few nanoseconds. In *run0* there appears to be memory of the ordered seed, since the distribution of bond directions in the simulation cell was higher along the simulation cell axes. The time required for the onset of crystallisation is also lower than in *runs1-3*, and the rate of crystallisation after onset is higher. Full crystallinity occurred after 1.2 ns in *run0*. After this time, *run1* was at 25%, *run2* at 15%, and *run3* at 20% crystallinity and there was no percolation in any of the three. In all simulations that crystallised fully, the final structures have “wrong” bonds that do not exist in the undistorted Yamada model¹¹. The number of wrong bonds is highest in the amorphous structures, and decreases during crystallisation. Nevertheless, the final structures have 0.1 – 0.3 wrong bonds/atom.

4 Concluding Remarks

Crystallisation occurs in most disordered systems on time scales that are far beyond the scope of density functional based calculations. Phase change materials used as optical storage and computer memory are exceptional in that the time scale (some nanoseconds) is accessible with modern supercomputers, and the results could provide insight into crystallisation in general. Nevertheless, DF/MD simulations on a nanosecond time scale with adequate sample sizes remain a great computational challenge. Here we have studied the early stages of crystallisation in GST-225 using samples with 460 atoms over simulation times of over 4 ns. In some cases, crystallisation has been promoted by inserting a small crystallite in the cell, and we have been able to follow the process in detail in all cases. The crystalline structures contain many “wrong bonds”, and Te atoms are located on both rock salt sublattices. The commonly accepted picture of a structure with a perfect Te sublattice and random occupancy of Ge, Sb, and vacancies on the other is a substantial oversimplification.

The memory of the order in *run0* remained after the seed was no longer evident, and the acceleration of crystallisation in an amorphous bit with a crystalline history should be a consideration in the design of future memory cells. The speed of crystallisation found in *run0* and the alignment of the final structure along the axes of the simulation cell were not found in simulations *runs1-3*. The starting configuration of the latter in each case was the amorphous structure found in Ref. 3, the only differences being in the initial velocity distributions at 600 K. These apparently small differences lead to large differences in the crystallisation process. Nevertheless, they involve many more atoms and much longer times than all previous DF studies of the process, and they raise questions about the findings of most, in particular those of a recent study⁶ that indicated that all cavities segregate

to the amorphous-crystalline boundary, leaving a cavity-free crystal. There is no evidence for this mechanism in any of our simulations.

The simulation trajectories show crystallisation directions that are unrelated to the axes of the simulation cell, and they show subcritical phases with ordered clusters of 10-50 atoms prior to the onset of crystallisation. Although the onsets differed, the speed of crystallisation from the subcritical phases is similar in all cases, and two of the simulations show multiple clusters and “polycrystalline” final structures. The final structure in all cases show the existence of low-frequency, localised vibrational modes that are not present in the original amorphous structures. Percolation initiates the rapid phase of crystallisation and is coupled to the directional p-type bonding in metastable GST-225. The apparent acceleration of crystallisation in a sample with an ordered history could lead to improved optical storage media.

Each simulation of 4 ns with a time step of ~ 3 fs requires over 1.3 million self-consistent density functional calculations of energies and forces for a sample of 460 atoms. Even using a computer with the performance of JUQUEEN, this is a task that demands both great computing *and* human resources.

Acknowledgements

We acknowledge gratefully computer time provided by the JARA-HPC Vergabegremium on the JARA-HPC partition of the supercomputer JUQUEEN at Forschungszentrum Jülich and for time granted on the supercomputer JUROPA at the Forschungszentrum Jülich.

References

1. M. Wuttig and N. Yamada, *Phase-change materials for rewriteable data storage*, Nature Mater. **6**, 824, 2007 and references therein.
2. J. Akola and R. O. Jones, *Binary alloys of Ge and Te: order, voids, and the eutectic composition*, Phys. Rev. Lett. **100**, 205502, 2008; *Density functional study of amorphous, liquid and crystalline $\text{Ge}_2\text{Sb}_2\text{Te}_5$: Homopolar bonds and/or AB alternation?* J. Phys.: Condens. Matter **20**, 465103, 2008.
3. J. Akola, R. O. Jones, S. Kohara, S. Kimura, K. Kobayashi, M. Takata, T. Matsunaga, R. Kojima, and N. Yamada, *Experimentally constrained density-functional calculations of the amorphous structure of the prototypical phase-change material $\text{Ge}_2\text{Sb}_2\text{Te}_5$* , Phys. Rev. B **80**, 020201(R), 2009, and references therein.
4. T. Matsunaga, J. Akola, S. Kohara, T. Honma, K. Kobayashi, E. Ikenaga, R. O. Jones, N. Yamada, M. Takata, and R. Kojima, *From local structure to nanosecond recrystallization dynamics in AgInSbTe phase change materials*, Nature Mater. **10**, 129, 2011.
5. J. Hegedüs and S. R. Elliott, *Microscopic origin of the fast crystallization ability of Ge–Sb–Te phase-change memory materials*, Nature Mater. **7**, 399, 2008.
6. T. H. Lee and S. R. Elliott, *Structural role of vacancies in the phase transition of $\text{Ge}_2\text{Sb}_2\text{Te}_5$ memory materials*, Phys. Rev. B **84**, 094124, 2011; *Ab initio computer simulation of the early stages of crystallization: Application to $\text{Ge}_2\text{Sb}_2\text{Te}_5$ phase-change materials*, Phys. Rev. Lett. **107**, 145702, 2011.

7. CPMD version 3.15. © IBM Corporation (1990-2012), MPI für Festkörperforschung, Stuttgart (1997-2001) (<http://www.cpmd.org/>).
8. J. P. Perdew, A. Ruzsinszky, G. I. Csonka, O. A. Vydrov, G. E. Scuseria, L. A. Constantin, X. Zhao, and K. Burke, *Restoring the density-gradient expansion for exchange in solids and surfaces*, Phys. Rev. Lett. **100**, 136406, 2008.
9. N. Troullier and J. L. Martins, *Efficient pseudopotentials for plane-wave calculations*, Phys. Rev. B **43**, 2006, 1991.
10. J. Kalikka, J. Akola, J. Larrucea, and R. O. Jones, *Nucleus-driven crystallization of amorphous $\text{Ge}_2\text{Sb}_2\text{Te}_5$: A density functional study*, Phys. Rev. B **86**, 144113, 2012.
11. N. Yamada, *Erasable phase-change optical materials*, MRS Bulletin **21**, 48, 1996.
12. P. J. Steinhardt, D. R. Nelson, and M. Rochetti, *Bond-orientational order in liquids and glasses*, Phys. Rev. B **28**, 784, 1983.
13. J. Kalikka, J. Akola, and R. O. Jones, *Simulation of crystallization in $\text{Ge}_2\text{Sb}_2\text{Te}_5$: A memory effect in the canonical phase-change material*, Phys. Rev. B **90**, 184109, 2014.
14. J. Orava, A. L. Greer, B. Gholipour, D. W. Hewak, and C. E. Smith, *Characteriation of supercooled liquid $\text{Ge}_2\text{Sb}_2\text{Te}_5$ and its crystallization by ultrafast-heating calorimetry*, Nature Mater. **11**, 279, 2012.